LBV nebulae in the Large Magellanic Cloud: exploring the dust content in the ALMA era

Claudia Agliozzo[1]

G. Umana[2], C. Trigilio[2], C. Buemi[2], A. Ingallinera[1], P. Leto[2], A. Noriega-Crespo[3]

1. Università degli studi di Catania
2. INAF-OACT
3. Spitzer Science Center-CALTECH

LMC as seen by Herschel (red 250 μm, green 100 μm) and Spitzer (blue 70 μm)

Image credit: ESA/NASA/JPL-Caltech/STScI

Luminous Blue Variable Stars

PROPERTIES

- **Post-MS**
  $M_{MS} > 22\ M_{\odot}$
- $L \sim 10^{5}$-$10^{6}\ L_{\odot}$
- **Variable**
- **Spectral type**
  O-B $(30\text{-}20\text{x}10^{3}\ K)$
  A-F $(10\text{-}8\text{x}10^{3}\ K)$

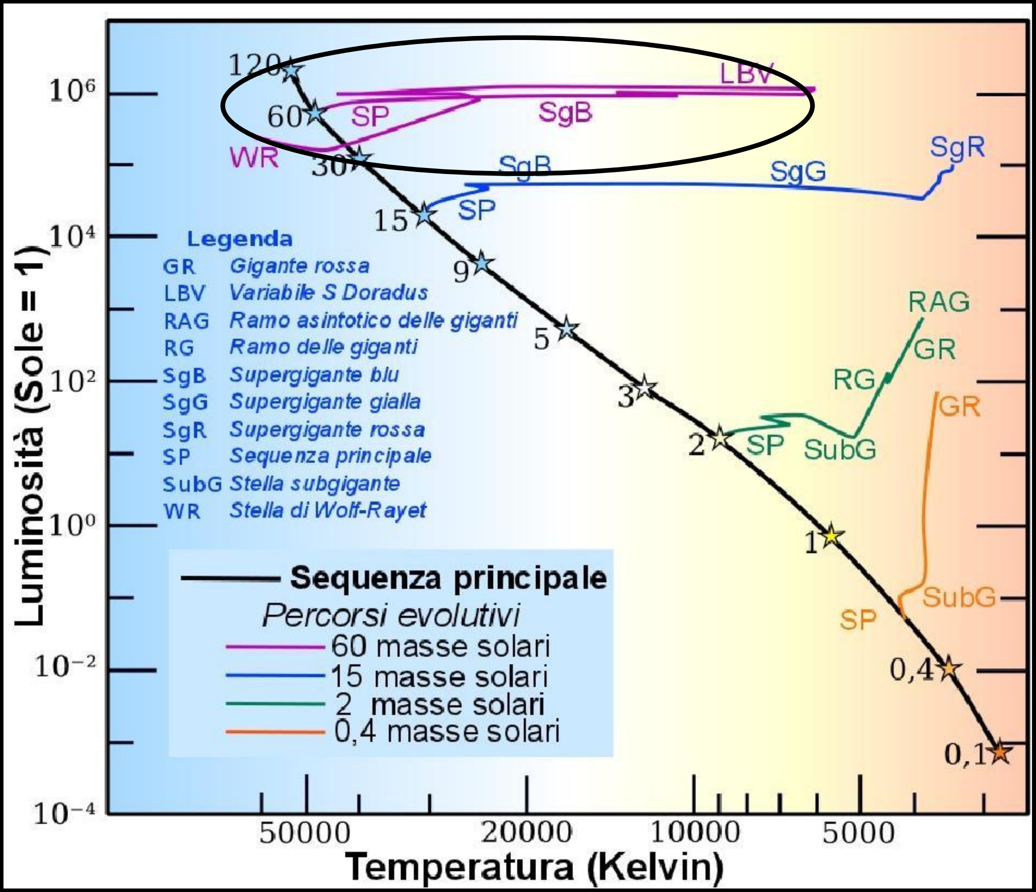

- $\dot{M} \sim 10^{-7} - 10^{-4}\, M_{\odot}\, yr^{-1}$
  (stellar wind or outburst) → **SN impostors**
- $t \sim 10^{4}\ yr$ → **Nebula ~ few** $M_{\odot}$

Luminous Blue Variable Stars

Rare objects (lifetime ~ 10^4-10^5 yr)

A recent census in the Milky Way reported:

12 confirmed LBVs

23 candidate LBVs

A few reported in nearby galaxies:

For ex. 22 objects in the Magellanic Clouds

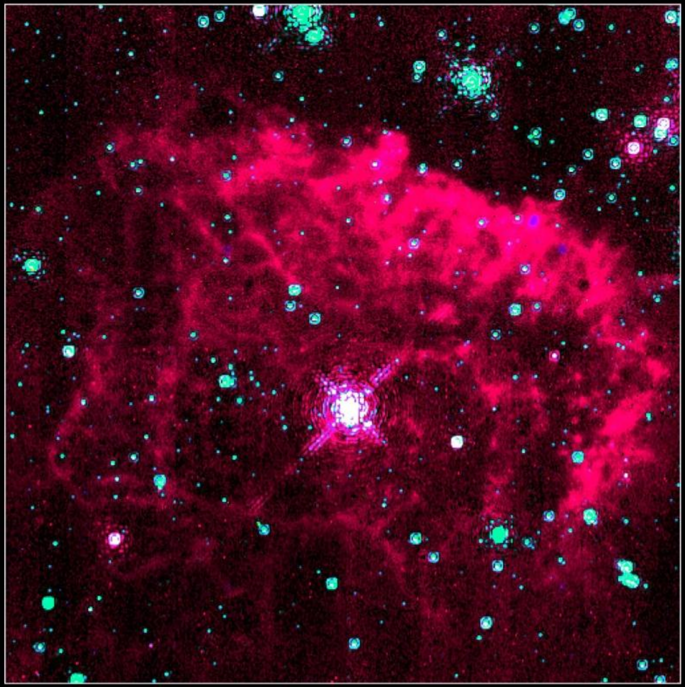

Pistol Star and Nebula
Hubble Space Telescope • NICMOS

PRC97-33 • ST ScI OPO • October 8, 1997 • D. Figer (UCLA) and NASA

Luminous Blue Variable Stars

Most interesting aspects

- Direct progenitors of Wolf-Rayet stars and core-collapse SN
- Provide enrichment of processed material and mechanical energy
- Dust producers in high-redshift galaxies?

Eta Carinae HST • WFPC2
PRC96-23a • ST ScI OPO • June 10, 1996
J. Morse (U. CO), K. Davidson, (U. MN), NASA

Luminous Blue Variable Stars

Open questions

- Mass-loss mechanisms (steady wind or violent eruption)
- Origin and shaping of the LBV nebulae
- Lifetime of the LBV phase
- Total mass lost during the LBV phase

The total mass lost is a fundamental parameter to test evolutionary models.

A multiwavelength approach...

A Galactic example: G79.29+0.46

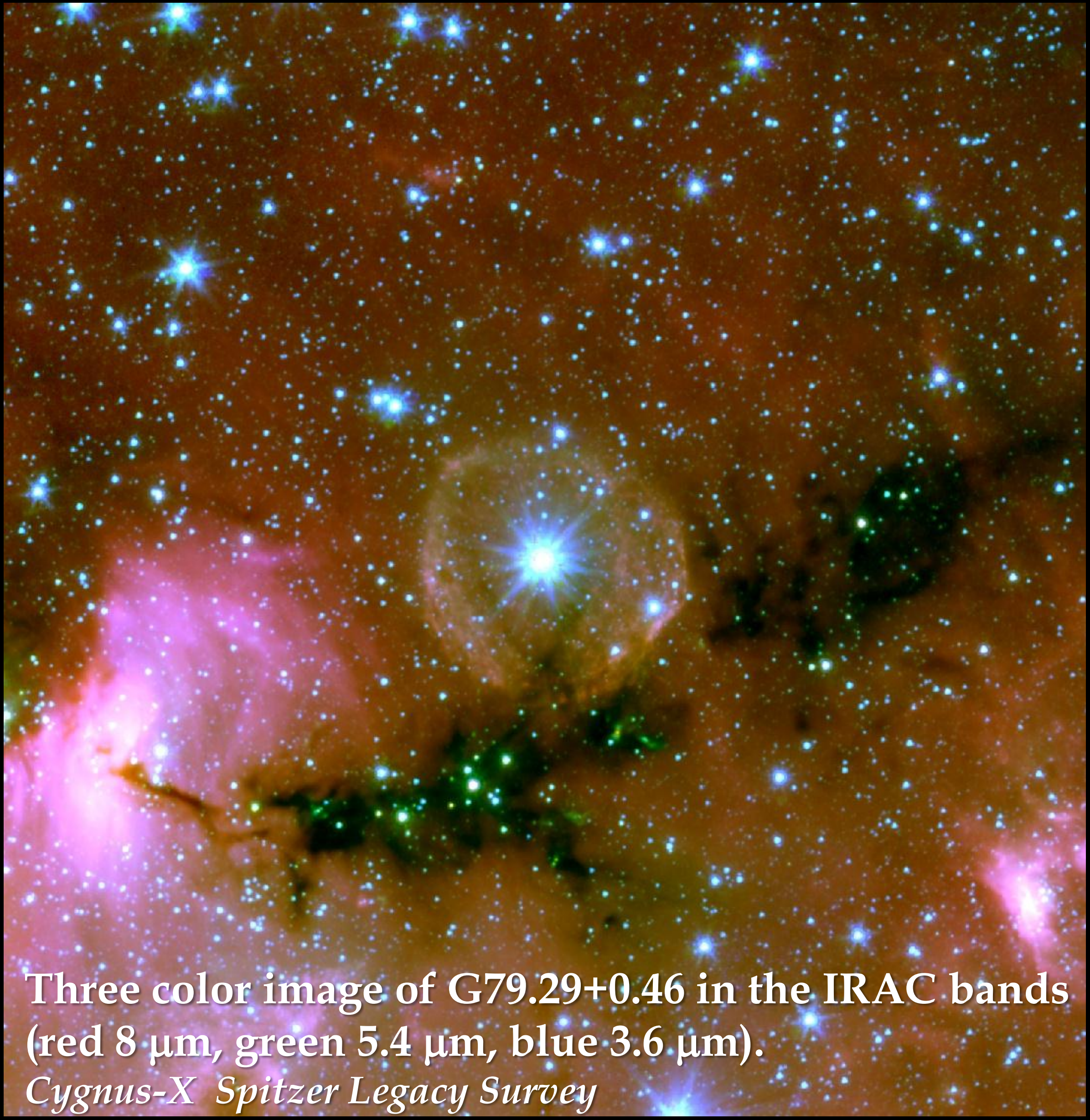

Three color image of G79.29+0.46 in the IRAC bands
(red 8 μm, green 5.4 μm, blue 3.6 μm).
Cygnus-X Spitzer Legacy Survey

A Galactic example: G79.29+0.46

D ~ 1.7 kpc

Multiple-shells i.d. different mass-loss episodes

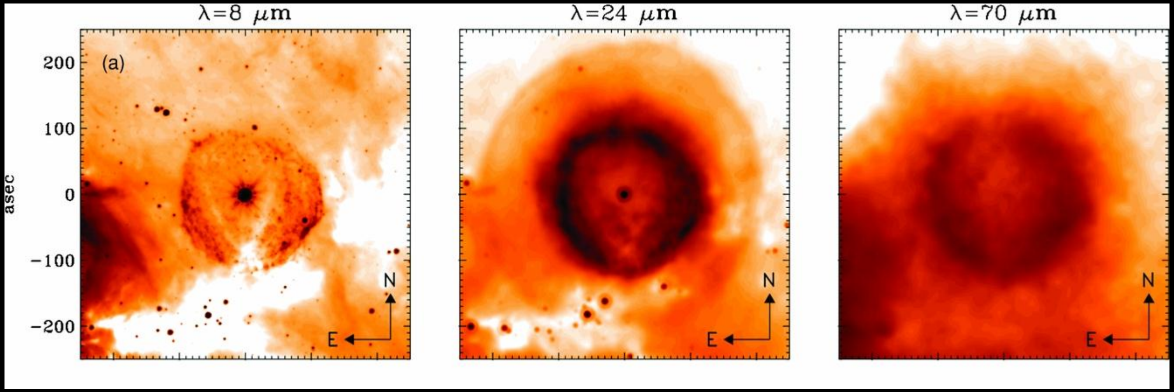

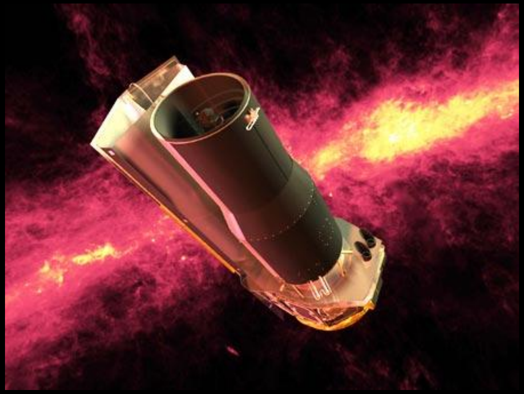

Spitzer observations
IRAC (3-8 μm)
MIPS (24, 70 μm)

T ~ 350 K
WARM DUST **(d_1 ~ 0.8 pc)**
COLDER DUST **(d_2 ~1.6 pc)**
T ~ 80-110 K

Umana et al. 2011, ApJL, 739, L11

A Galactic example: G79.29+0.46

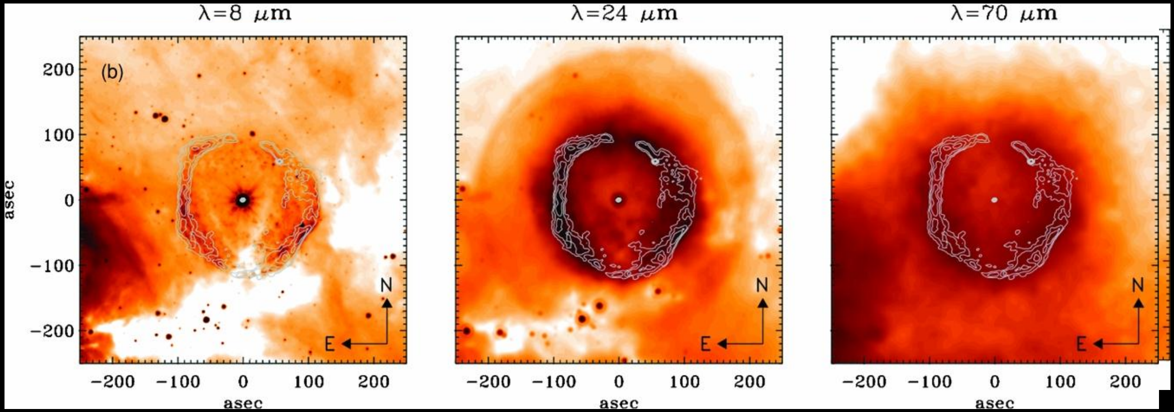

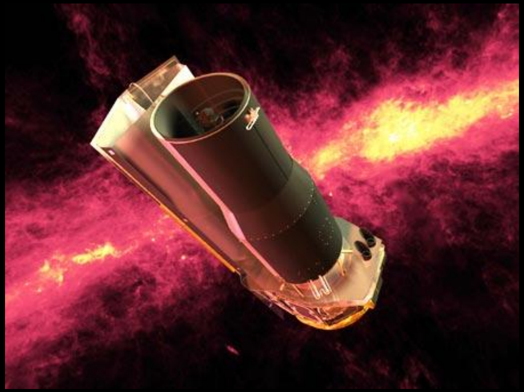

EVLA observations

1,10 June 2010
Config. D, Band L+C

IONIZED GAS

1, 5 December, 2010
Config. C, Band L+C

Umana et al. 2011, ApJL, 739, L11
Agliozzo et al. 2012, in preparation

A Galactic example: G79.29+0.46

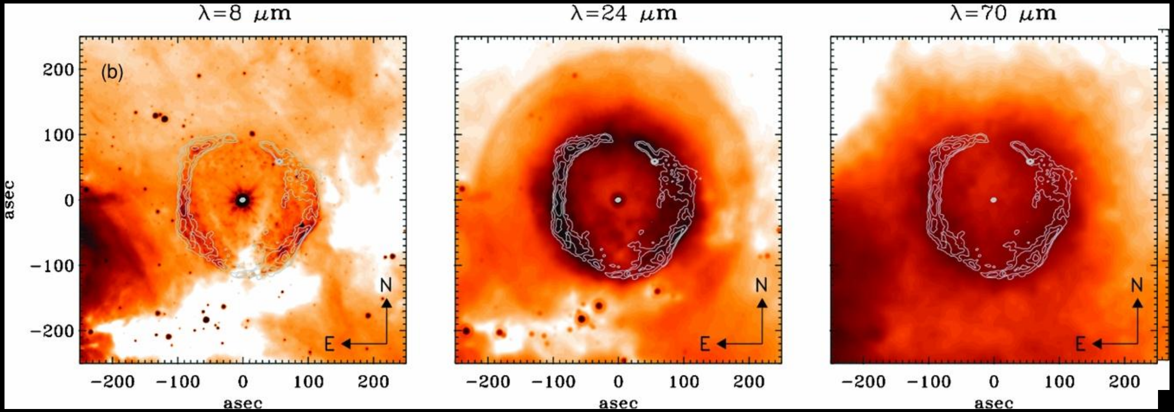

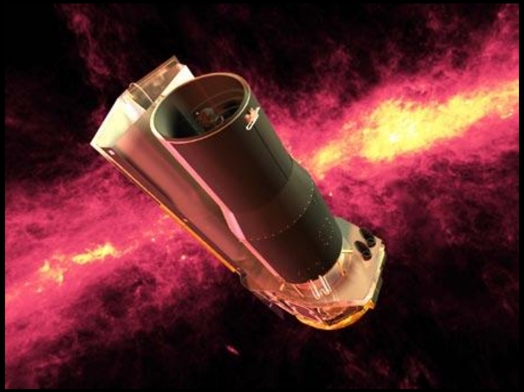

IONIZED GAS and DUST coexist

$\dot{M} \sim 5 \times 10^{-7}\ M_{\odot} yr^{-1}$

Umana et al. 2011, ApJL, 739, L11
Agliozzo et al. 2012, in preparation

A Galactic example: G79.29+0.46

Kinematical Age

$v_{exp} = 30$ km s^{-1}
$t_1 = 2.7 \times 10^4$ yr
$t_2 = 5.4 \times 10^4$ yr

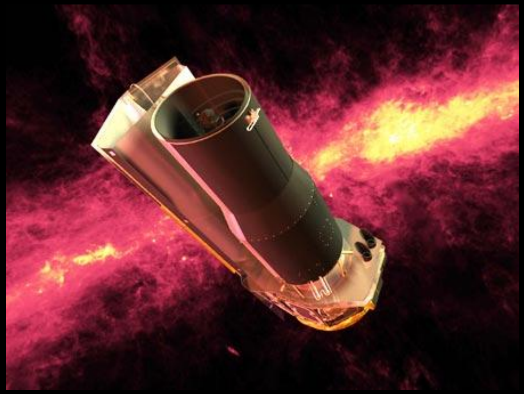

GREY: EVLA 6 cm
RED: Spitzer 24 μm

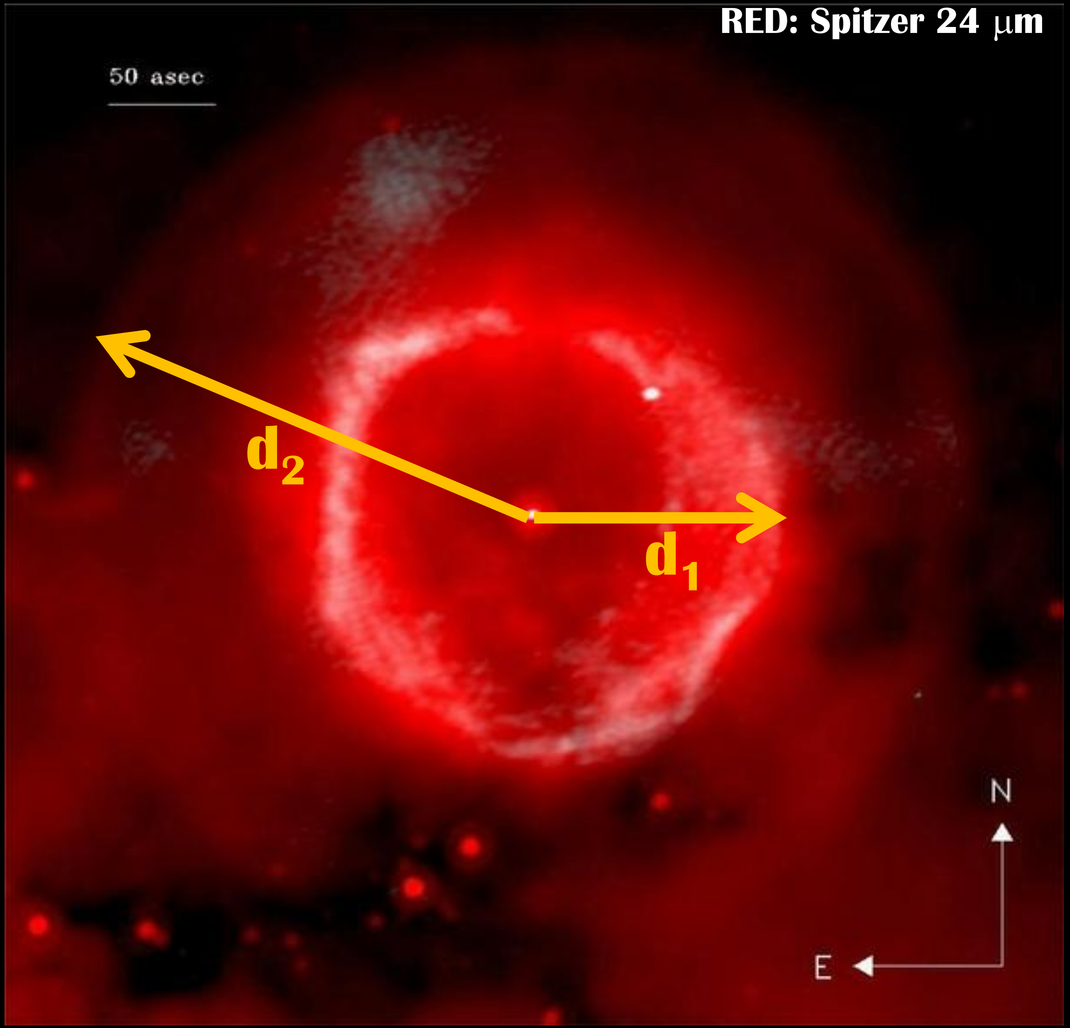

Umana et al. 2011, ApJL, 739, L11

LBV Nebulae in the Large Magellanic Cloud

Smith & Owocki 2006, ApJ, 645, L45:
LBV extreme mass-loss via eruptive episodes, driven by metallicity independent mechanisms.

LBVs important in the evolution of early universe massive stars.

LMC: laboratory to test if LBV is a metallicity independent phenomenon (D ~ 48.5 kpc , $Z_{LMC} \sim {}^{1}/_{2}\, Z_{\odot}$).

HST detections of LBV nebulae in the LMC

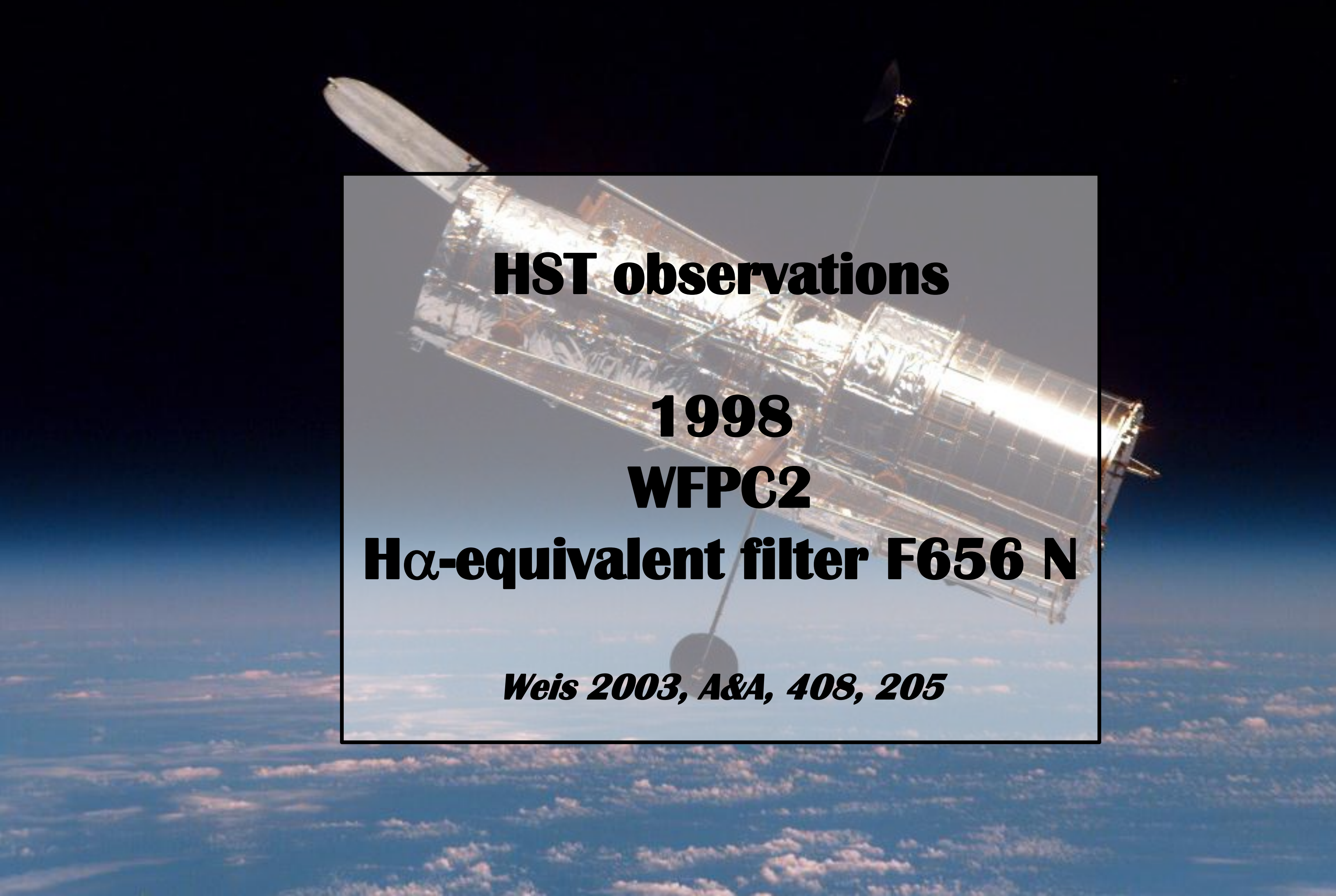

HST detections of LBV nebulae in the LMC

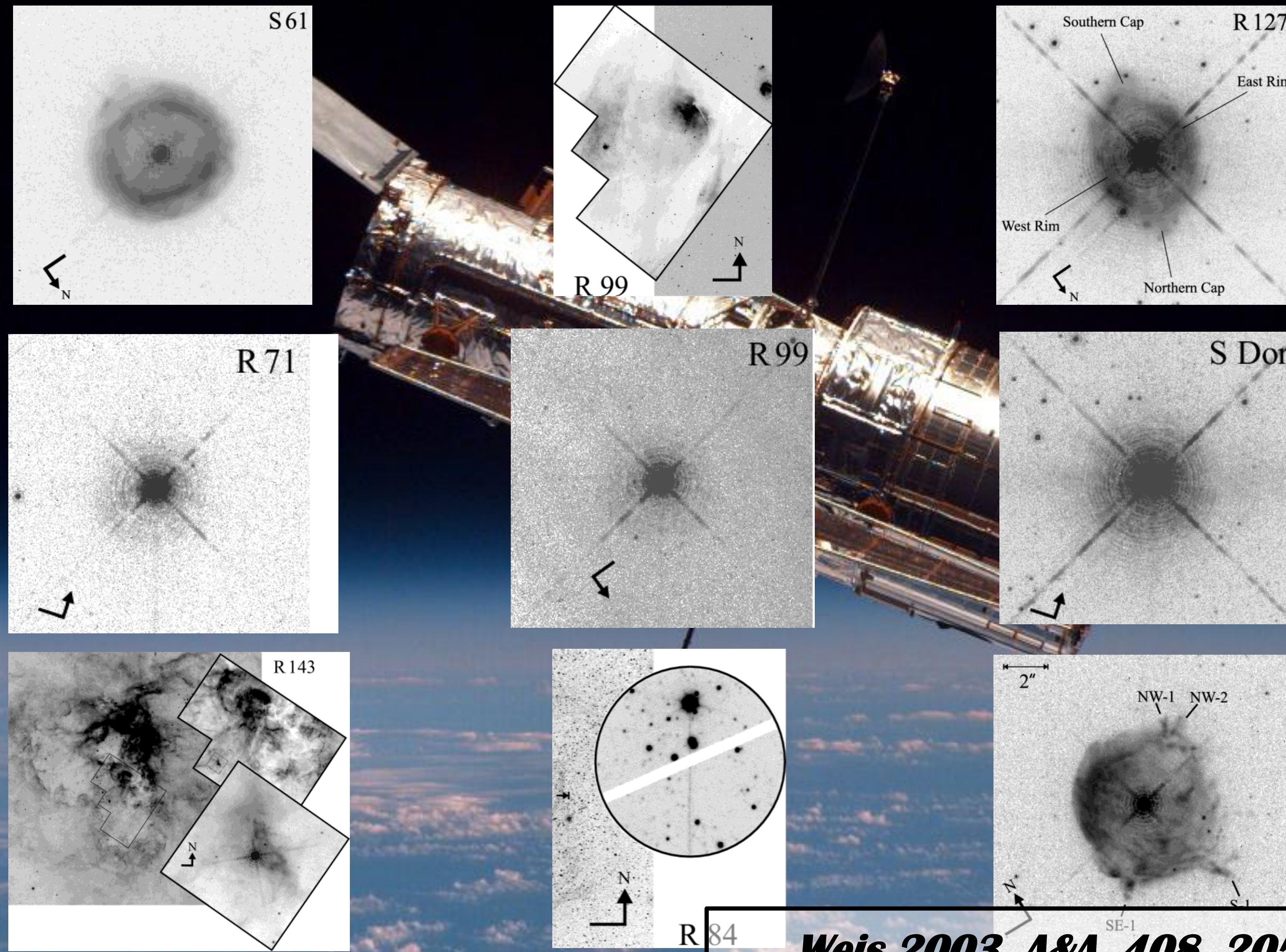

Weis 2003, A&A, 408, 205

HST detections of LBV nebulae in the LMC

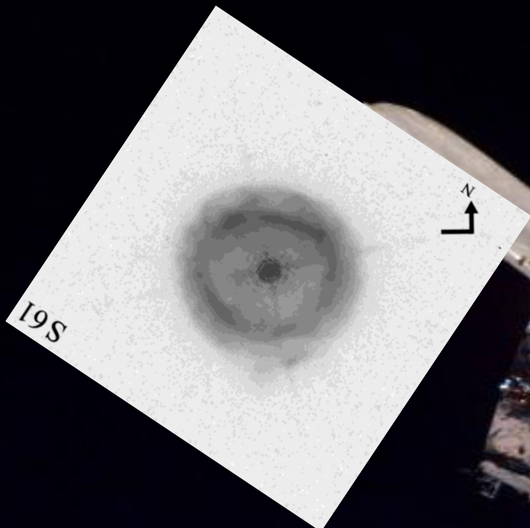

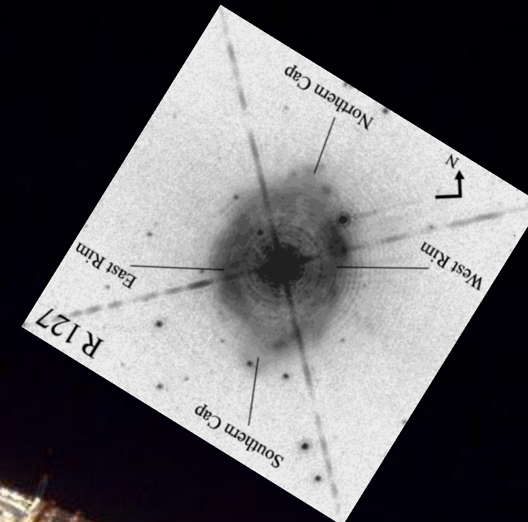

$$S_{\nu} = 8.81 \times 10^{6} T_e^{0.53} \nu^{-0.1} YF(H\alpha)$$

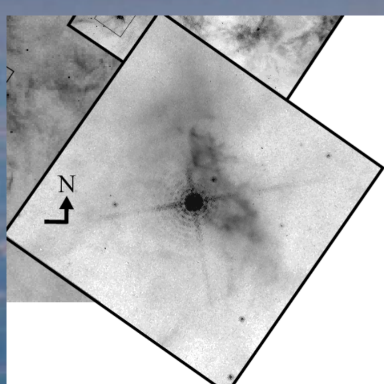

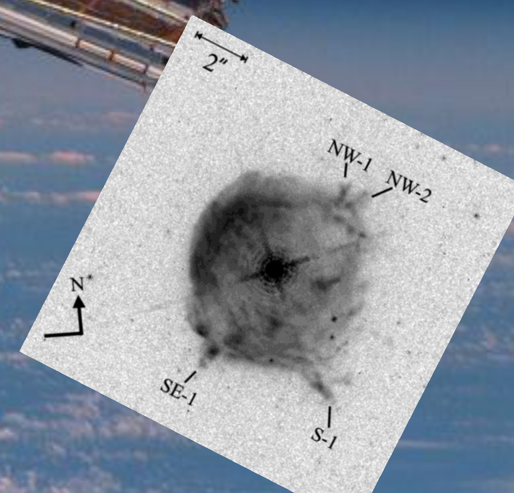

HST detections of LBV nebulae in the LMC

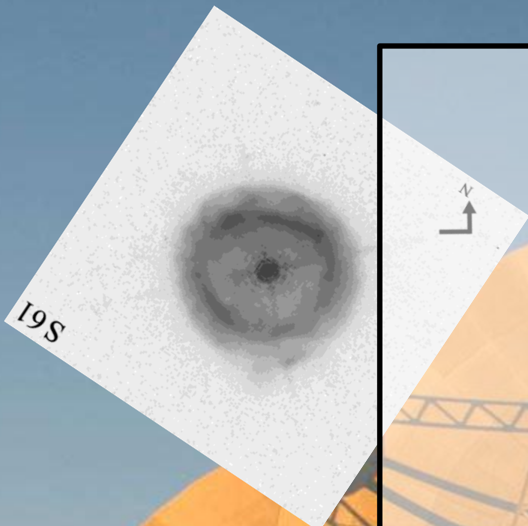

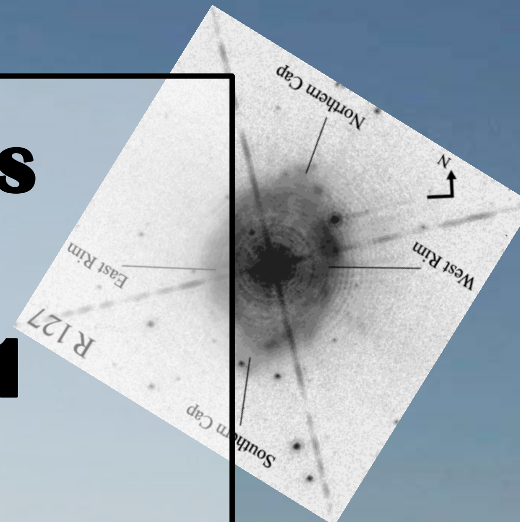

ATCA observations

18-20 April, 2011
Config. 6km
Band 3+6 cm

20-22 January, 2012
Config. 6km
Band 15 mm

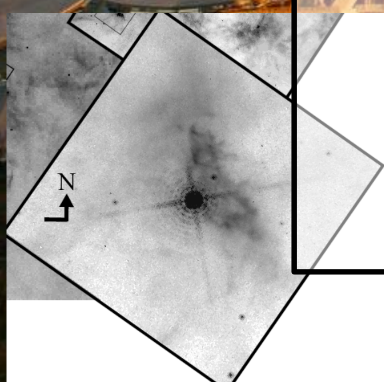

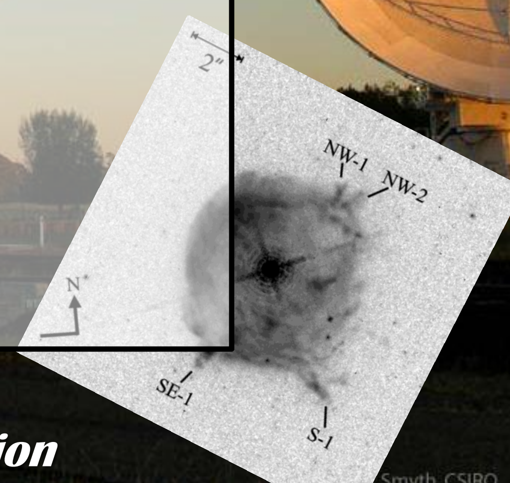

Agliozzo et al. 2012, in preparation

Smyth, CSIRO

First radio detections of LBV nebulae in the LMC

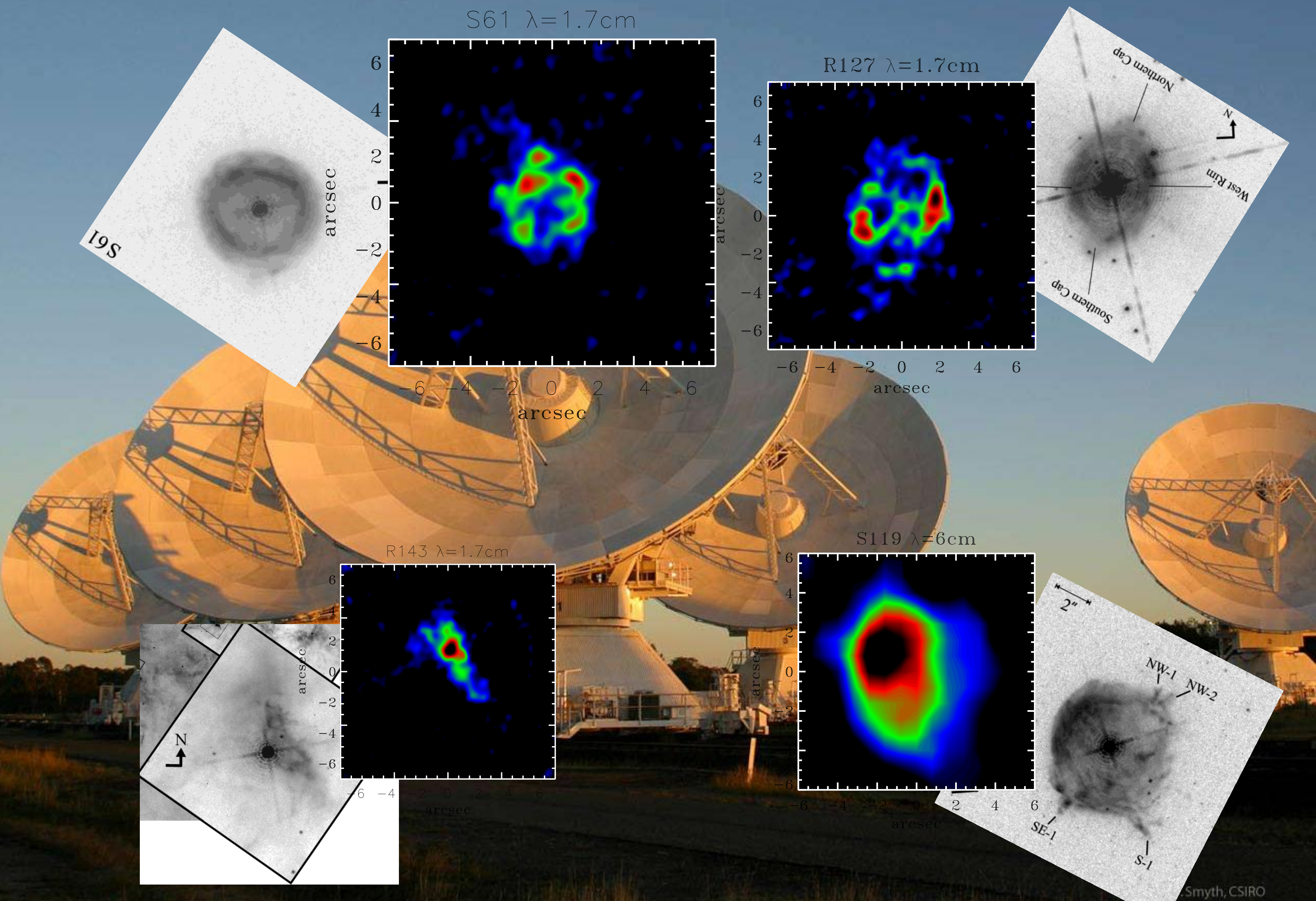

An example: R127

Beam = 0.8”x0.7”

RMS = 0.01 mJy/beam

I_{MAX} = 0.13 mJy/beam

F_{TOT} = 2.5 ± 0.2 mJy

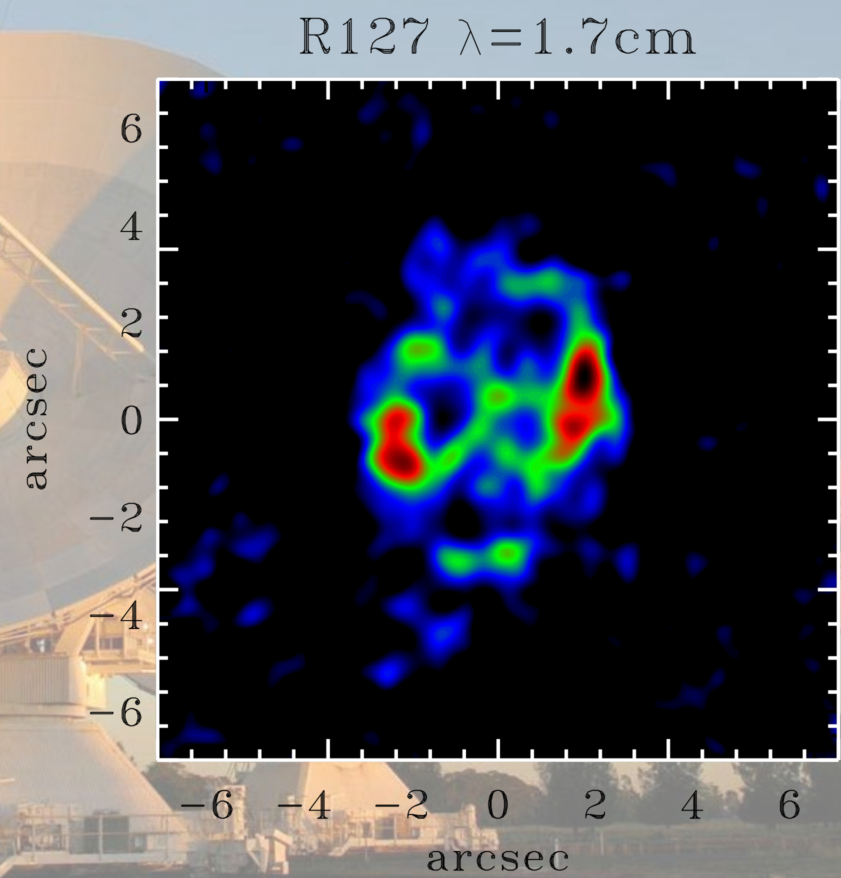

An example: R127

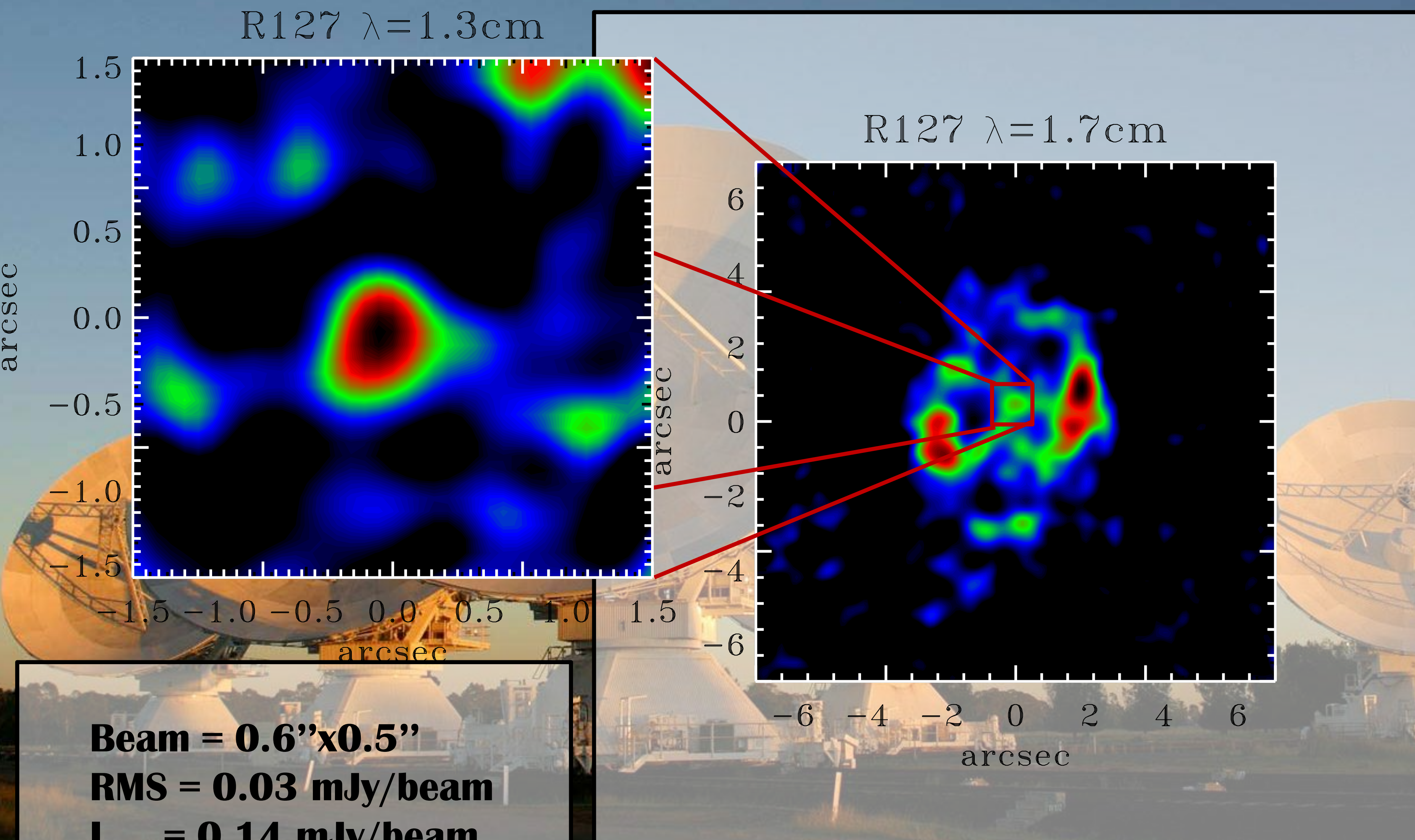

Beam = 0.6”x0.5”
RMS = 0.03 mJy/beam
I_{MAX} = 0.14 mJy/beam

An example: R127

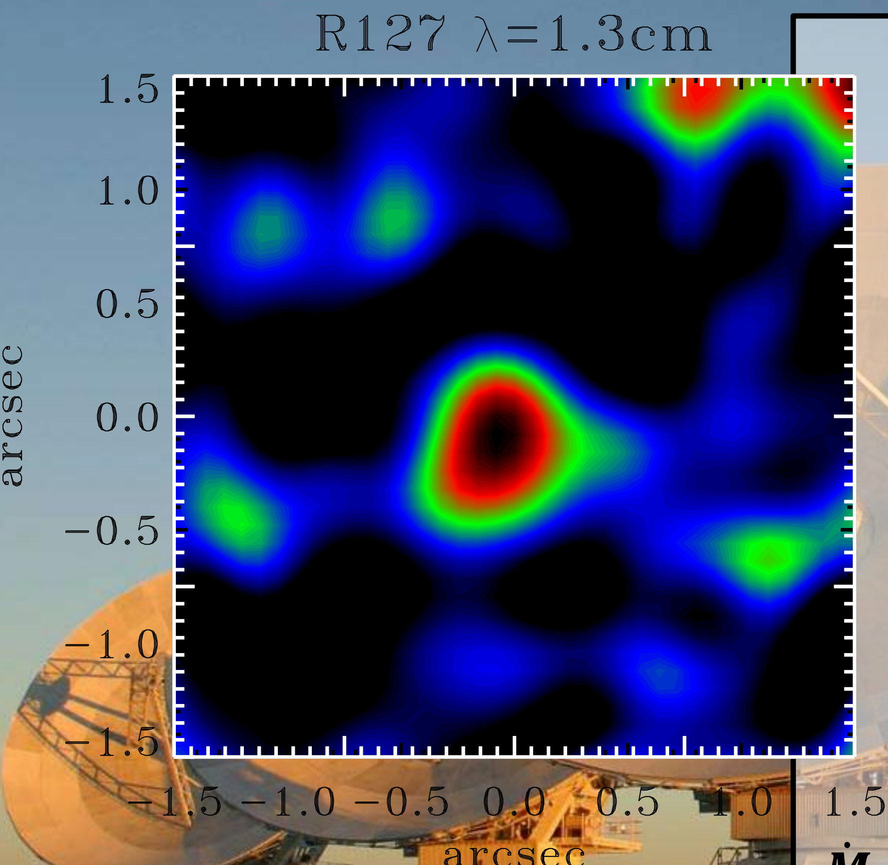

Beam = 0.6”x0.5”
RMS = 0.03 mJy/beam
I_{MAX} = 0.14 mJy/beam

Physical properties

F(1.3cm)=0.14 mJy

$\dot{M} \sim 2 \times 10^{-5}\, M_\odot\, yr^{-1}$

Current-day mass-loss

$$\dot{M} = 6.7 \times 10^{-4}\, v_{wind}\, F^{3/4} D^{3/2} (\nu \times gff)^{-0.5}$$

An example: R127

Physical properties

$n_e \sim 100\ \mathrm{cm}^{-3}$
$M_{ionized} = 1.2\ M_\odot$
$t_{nebula} = 2 \times 10^4$ yr
$F_{UV} = 2 \times 10^{46}\ s^{-1}$
Spectral Type > B1

$$\tau_{ff} = 8.24 \times 10^{-2} T_e^{-1.53} \nu^{-2,1} EM$$

$$EM = \int n_e^2\, dl$$

$$F_{UV} = \frac{M_{ionized} \beta_2 n_e}{m_p}$$

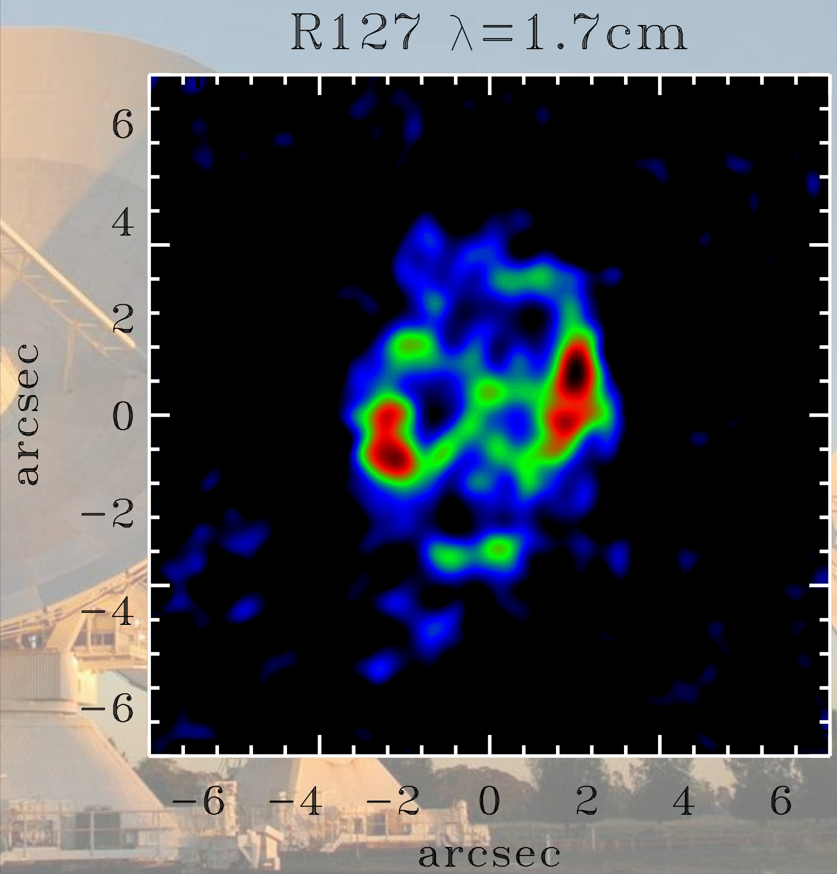

Evidence of dust

Comparison with Hα

$$S_\nu = 8.81 \times 10^6 T_e^{0.53} \nu^{-0.1} \mathrm{YF(H\alpha)}$$

Intrinsic extinction

$$\frac{S_\nu(obs)}{S_\nu(exp)} = e^{\tau_{H\alpha}}$$

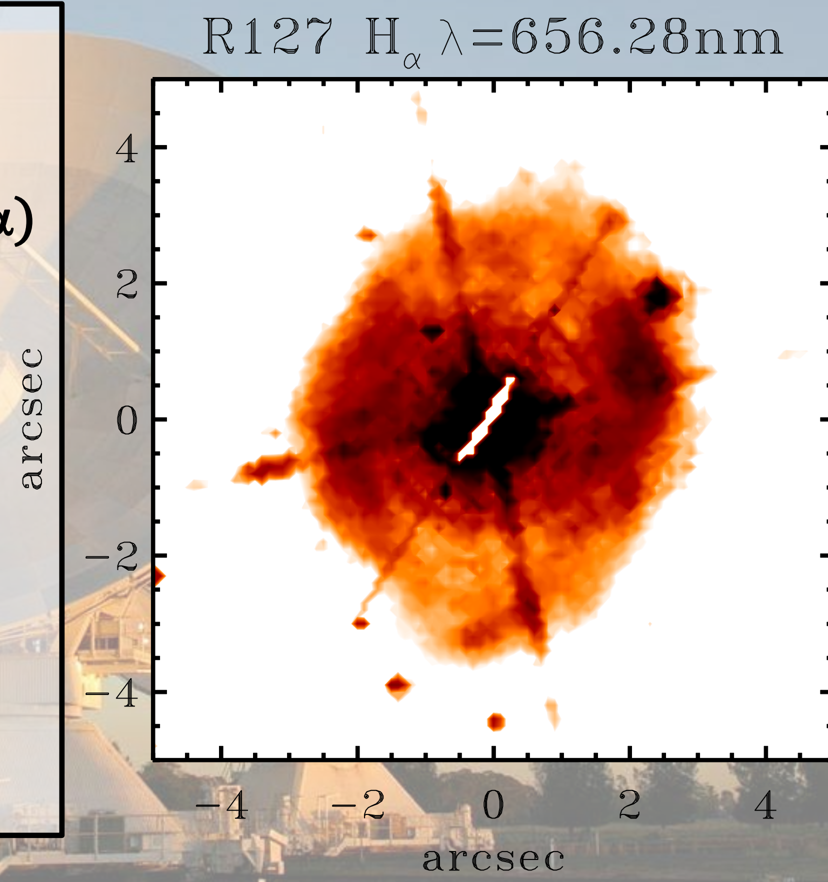

Evidence of dust

Comparison with Hα

$$S_\nu = 8.81\times 10^6 T_e^{0.53} \nu^{-0.1} YF(H\alpha)$$

Intrinsic extinction

$$\frac{S_\nu(obs)}{S_\nu(exp)} = e^{\tau_{H\alpha}}$$

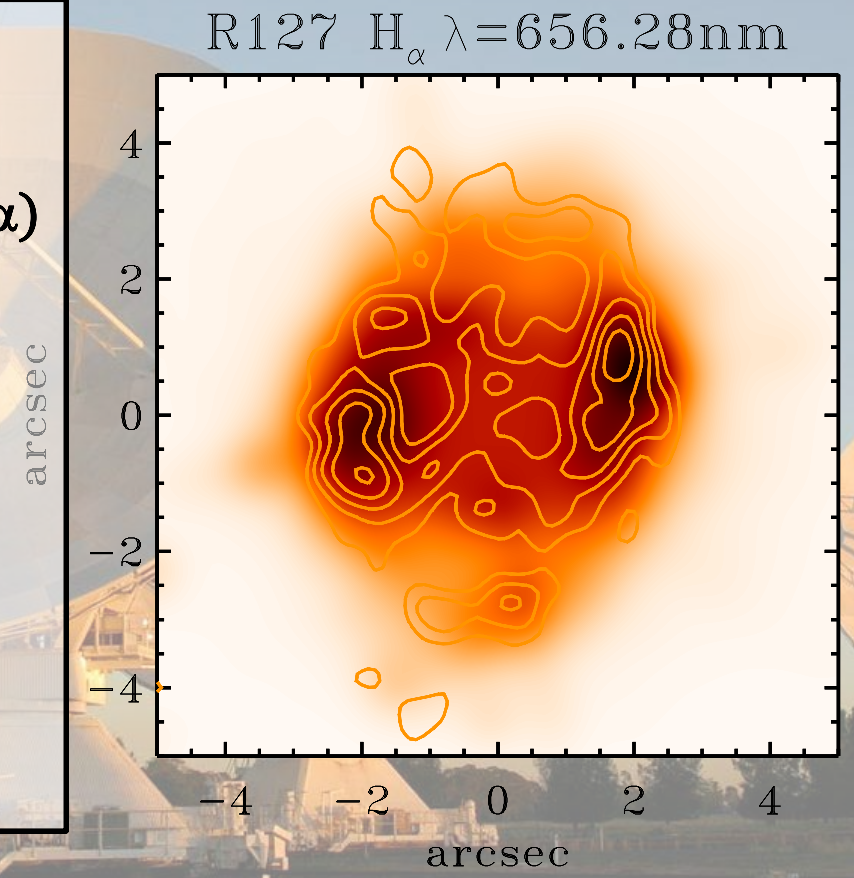

Evidence of dust

Comparison with Hα

$$S_\nu = 8.81\times 10^6 T_e^{0.53} \nu^{-0,1} \mathrm{YF(H\alpha)}$$

Intrinsic extinction

$$\frac{S_\nu(obs)}{S_\nu(exp)} = e^{\tau_{H\alpha}}$$

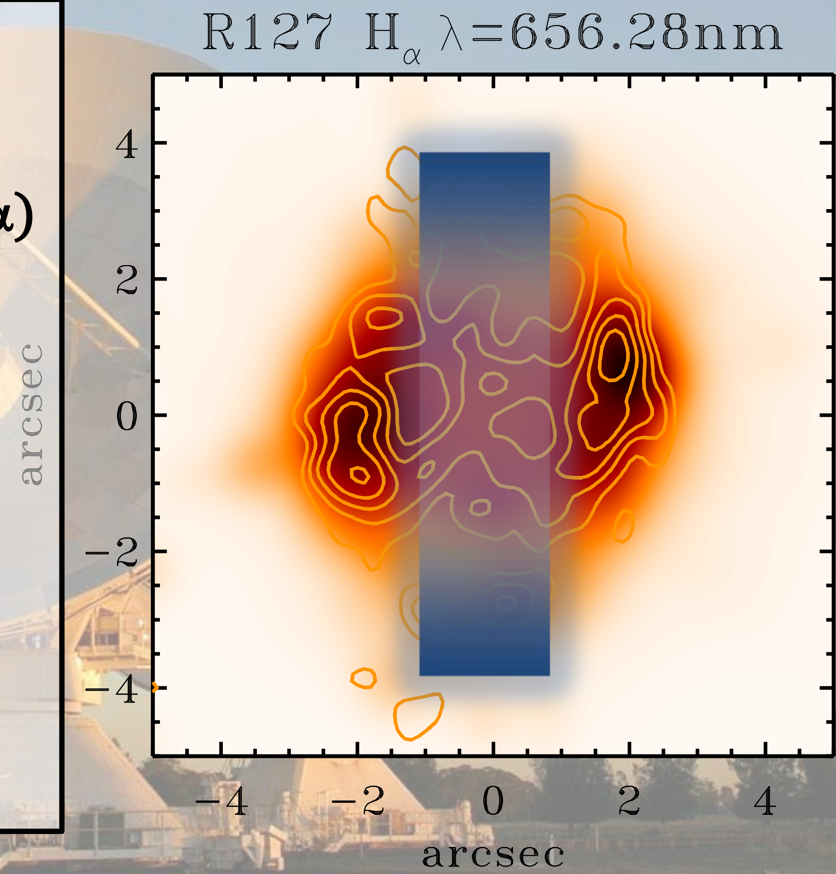

Evidence of cold dust in MCs LBV

R71

Spitzer (IRAC+MIPS)

Herschel (PAC+SPIRE)

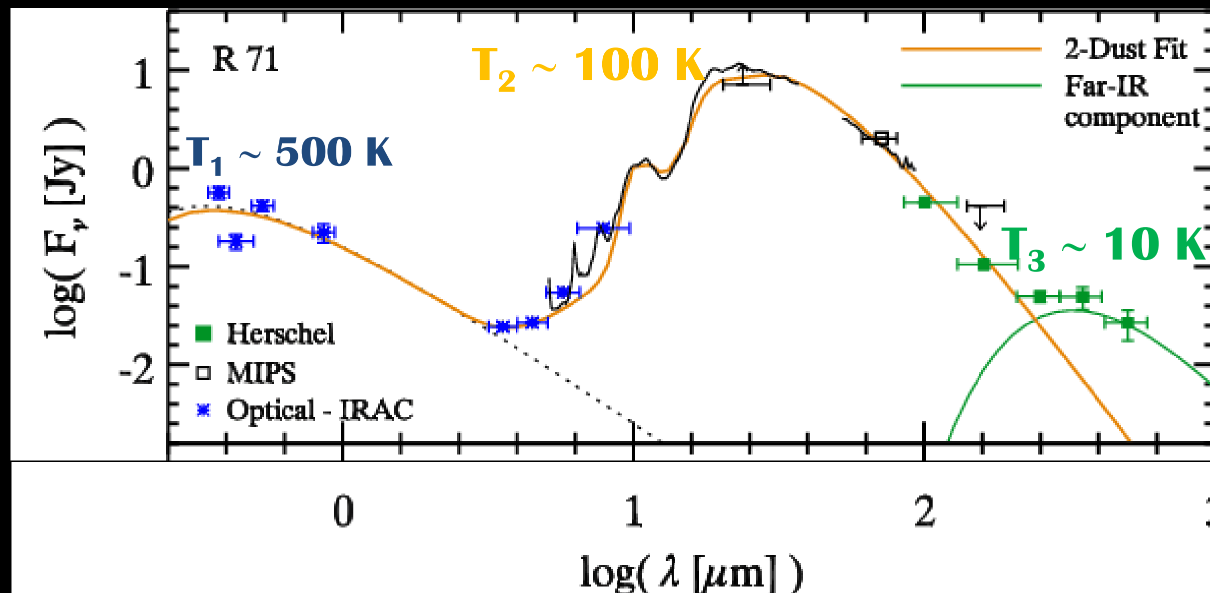

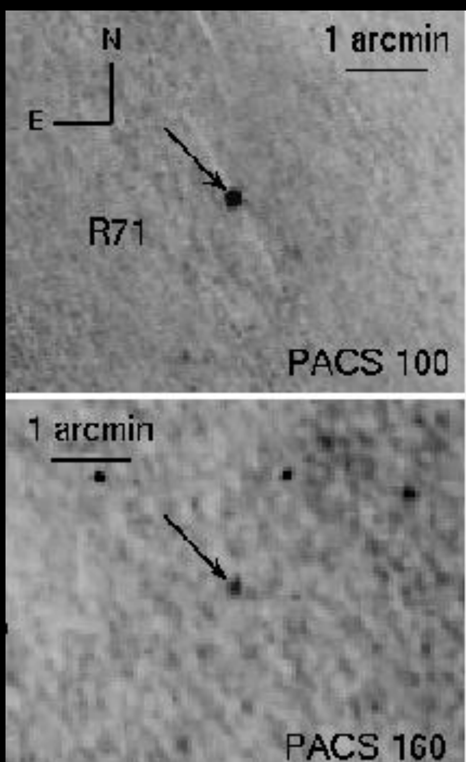

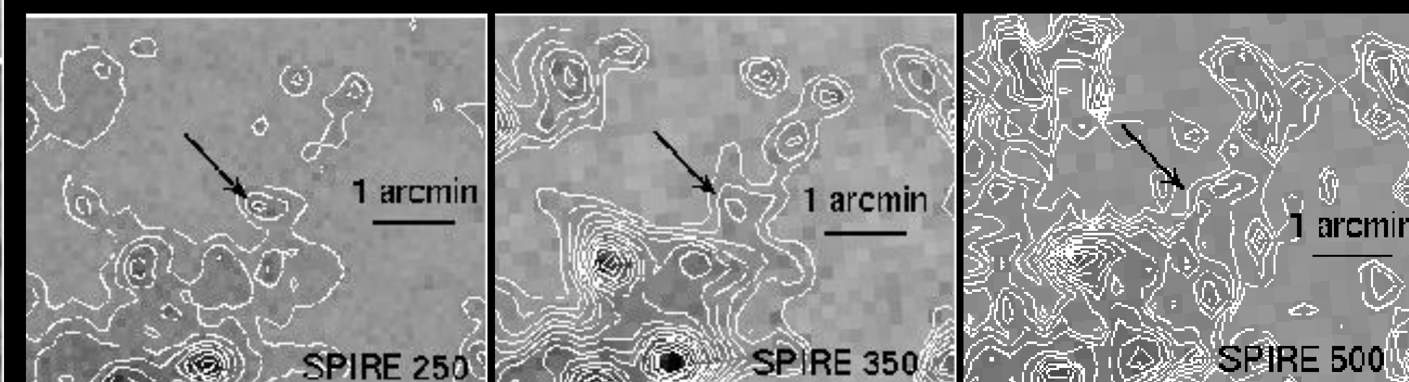

Boyer et al. 2010, A&A, 518, L142

Exploring the dust components with ALMA

Dust torus (carbonaceous)

$$B(T = 100\ K)$$

$$\tau_{ALMA} = \frac{\kappa_{ALMA}}{\kappa_{H_\alpha}} \tau_{H_\alpha}$$

$$I_{ALMA} = B(T = 100\ K) \times \tau_{ALMA}$$

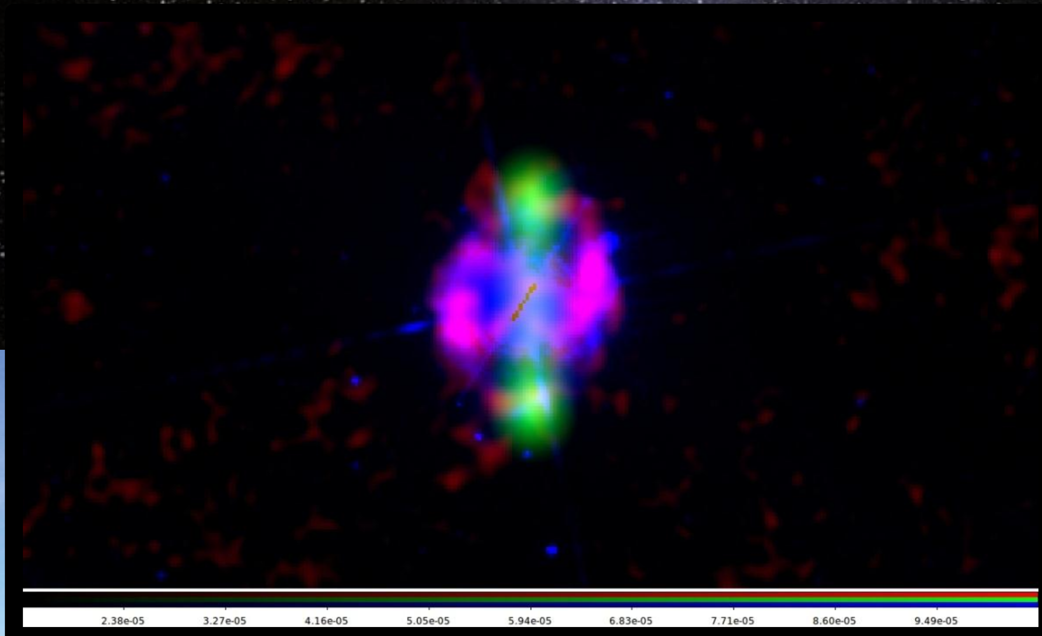

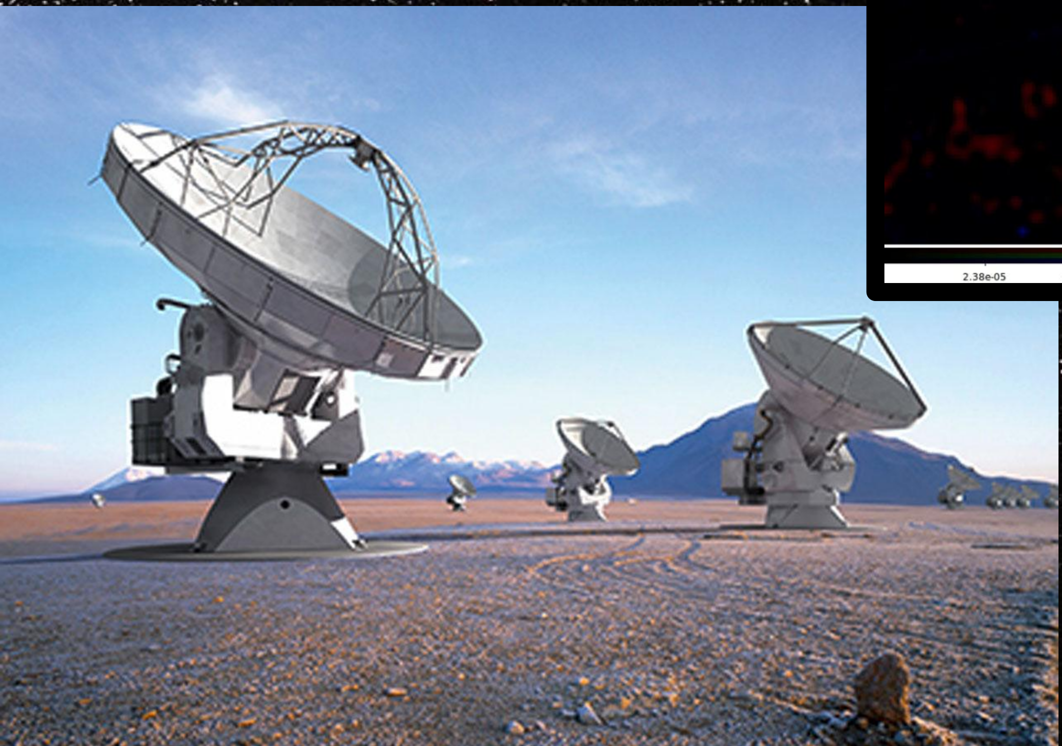

Exploring the dust components with ALMA

Band	Frequency [GHz]	Angular Resolution [“]	Maximum Scale [“]	T_{bc} [mK]	Flux [mJy]	T_{bl} [K]	Field of View [“]
Properties of the Compact Configuration (baselines of ~18 m to ~125 m)							
3	100	5.3	21	0.65	0.14	0.030	62
6	230	2.3	9	1.0	0.20	0.029	27
7	345	1.55	6	1.8	0.37	0.043	18
9	675	0.80	3	15	3.2	0.27	9
Properties of the Extended Configuration (baselines of ~36 m to ~400 m)							
3	100	1.56	10.5	7.6	0.14	0.35	62
6	230	0.68	4.5	11	0.20	0.34	27
7	345	0.45	3.0	20	0.37	0.50	18
9	675	0.23	1.5	175	3.2	3.1	9

Table 2. Properties of ALMA Cycle 0 Array Configurations

Exploring the dust components with ALMA

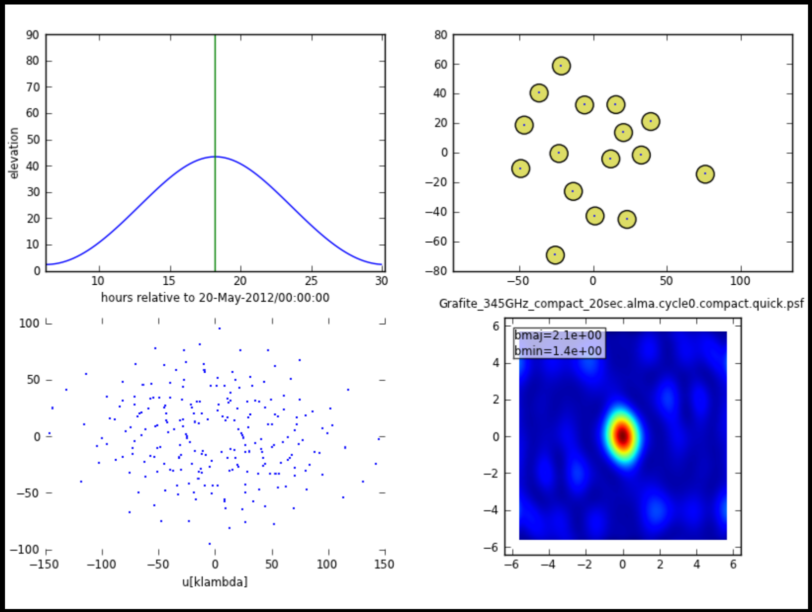

Band 7 (345 GHz)
Bandwidth 7.5 GHz
Config. Compact

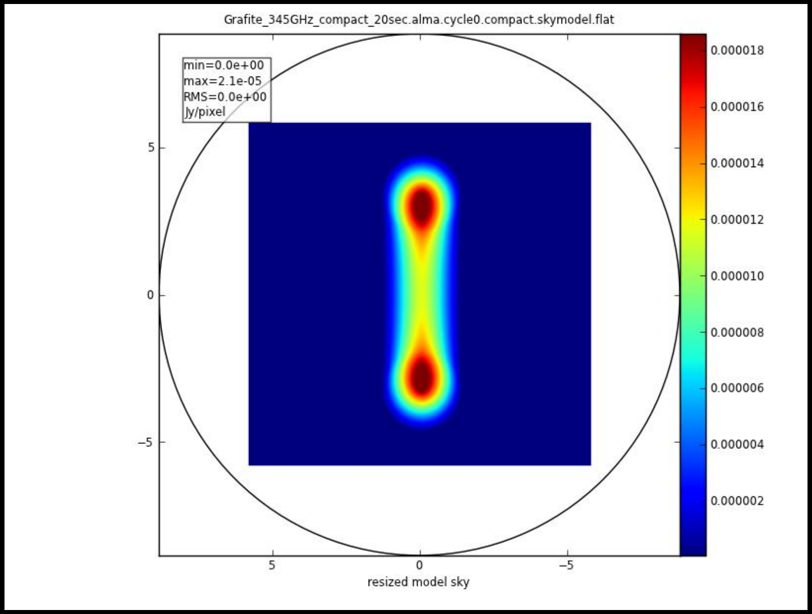

I = 0.02 mJy/pixel (pixel=0.1")
Beam 1.55"x1.55"
I = 5.6 mJy/Beam
Time on source = 20 s (3σ)

Exploring the dust components with ALMA

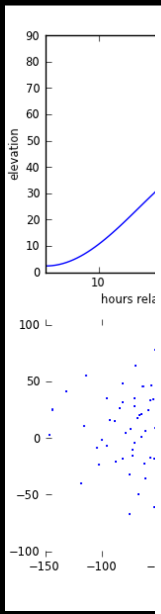

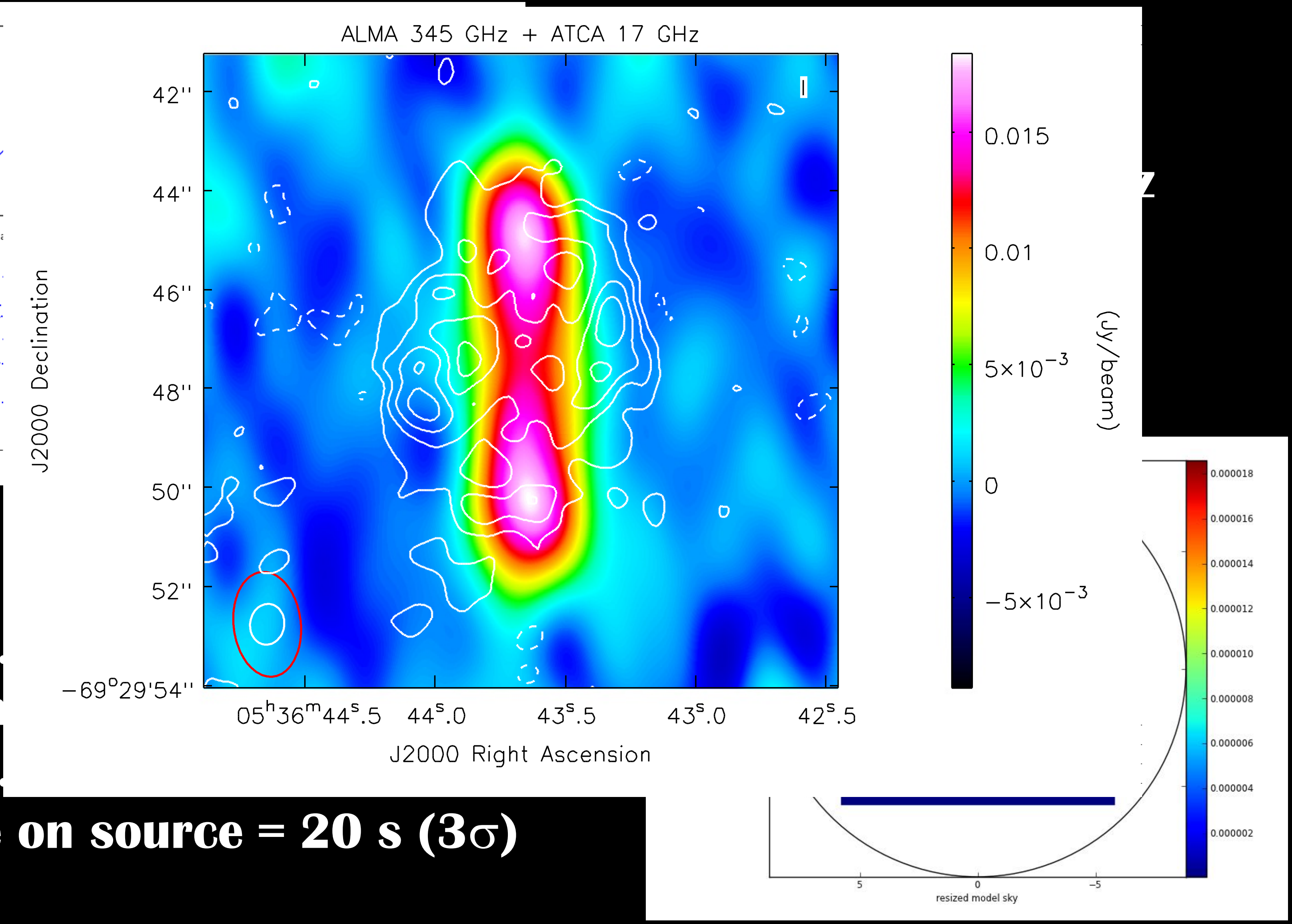

I = 0.

Bean

I = 5.

Time on source = 20 s (3σ)

Exploring the dust components with ALMA

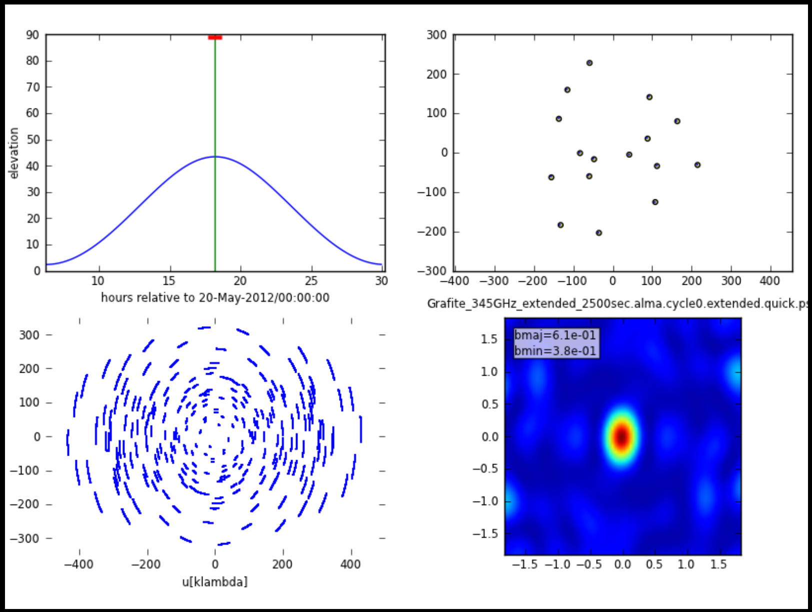

Band 7 (345 GHz)
Bandwidth 7.5 GHz
Config. Extended

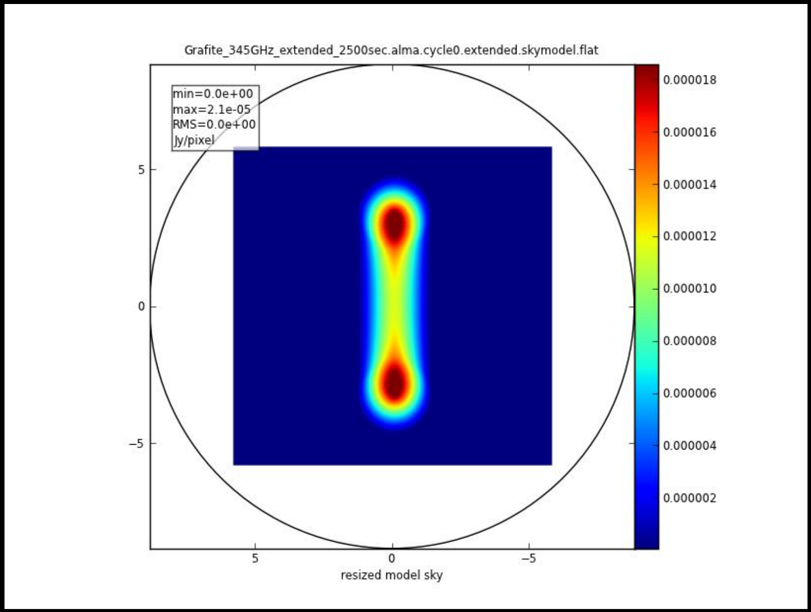

I = 0.02 mJy/pixel (pixel=0.1'')
Beam 0.45''x0.45''
I = 0.5 mJy/Beam
Time on source = 40 min (3σ)

Exploring the dust components with ALMA

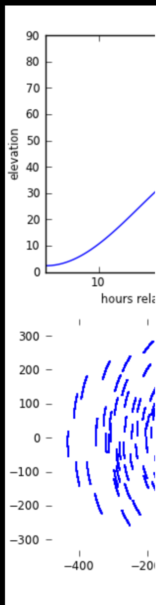

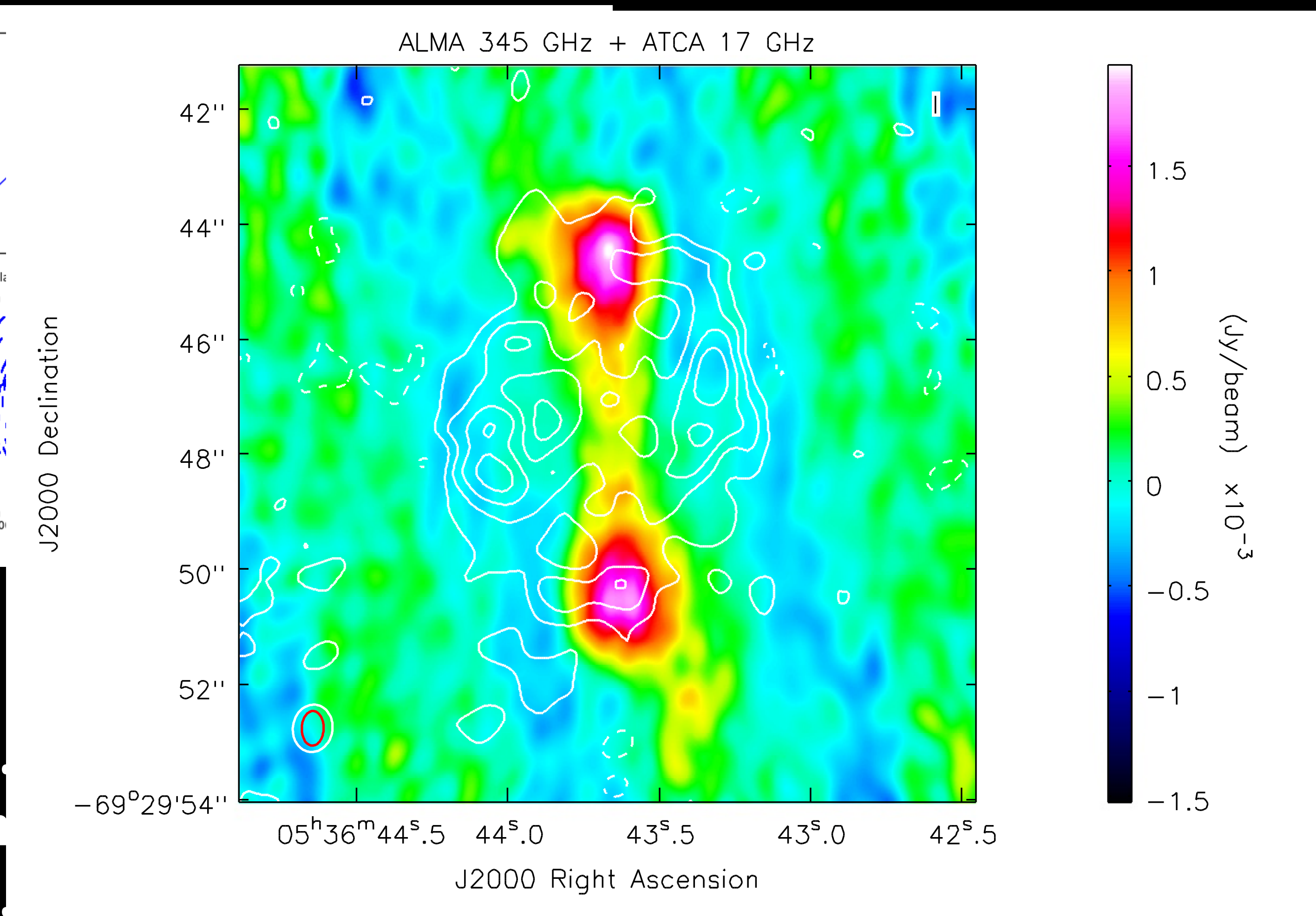

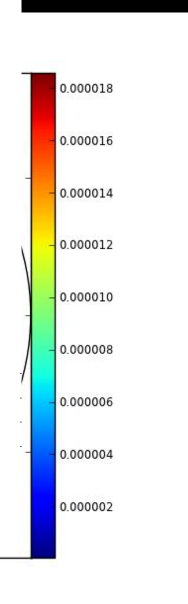

z

I = 0.

Bean

I = 0.

Time on source = 40 min (3σ)

Analysis of the dust

$$\frac{I_{700GHz}}{I_{345GHz}} = e^{-h(700-345)/KT}\left(\frac{345}{700}\right)^3\frac{\tau_{700}}{\tau_{345}}$$

$$I_\nu \approx B_\nu(T)\,\tau_\nu$$

$$\tau = \kappa_{dust}\rho_{dust} l$$

$$\int \rho_{dust}\, l\, dA = M_{dust}$$

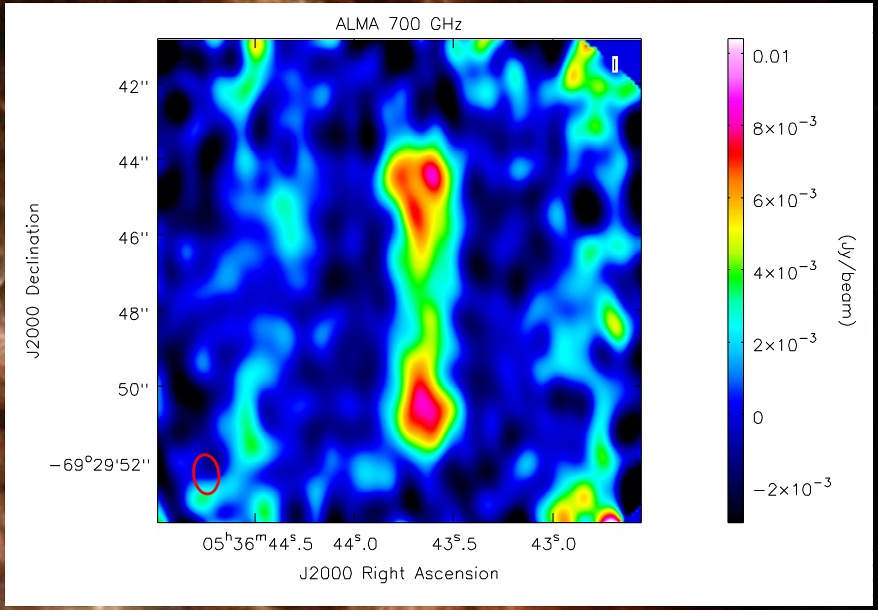

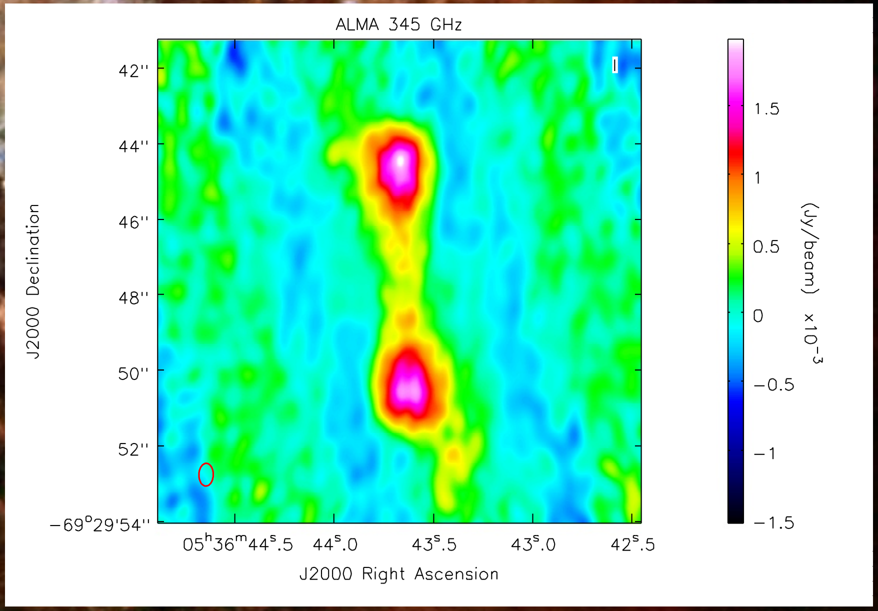

Conclusion

- **Multiwavelengths (ALMA+ATCA) – different CSE components**

- **Morphology of ionized gas (ATCA) and dust (ALMA)**

- $M_{nebula} = M_{dust} + M_{neutral\ gas} + M_{ionized\ gas}$

- **Current-day Mass-Loss + Kinematical Age of the nebulae**